ELSEVIER

Contents lists available at ScienceDirect

# **Environmental Pollution**

journal homepage: www.elsevier.com/locate/envpol





# Pre-differentiation exposure of PFOA induced persistent changes in DNA methylation and mitochondrial morphology in human dopaminergic-like neurons<sup>★</sup>

Han Zhao <sup>a</sup>, Junkai Xie <sup>a</sup>, Shichen Wu <sup>a</sup>, Oscar F Sánchez <sup>a</sup>, Xinle Zhang <sup>a</sup>, Jennifer L. Freeman <sup>b,c</sup>, Chongli Yuan <sup>a,c,\*</sup>

- <sup>a</sup> Davidson School of Chemical Engineering, Purdue University, West Lafayette, IN, 47907, USA
- <sup>b</sup> School of Health Sciences, Purdue University, West Lafayette, IN, 47907, USA
- <sup>c</sup> Purdue University Center for Cancer Research, West Lafayette, IN, 47907, USA

### ARTICLE INFO

Keywords:
PFOA exposure
PFAS exposure
DNA methylation
Mitochondrion
Epigenome
Dopaminergic neuron

### ABSTRACT

Perfluorooctanoic acid (PFOA) is abundant in environment due to its historical uses in consumer products and industrial applications. Exposure to low doses of PFOA has been associated with various disease risks, including neurological disorders. The underlying mechanism, however, remains poorly understood. In this study, we examined the effects of low dose PFOA exposure at 0.4 and 4  $\mu$ g/L on the morphology, epigenome, mitochondrion, and neuronal markers of dopaminergic (DA)-like SH-SY5Y cells. We observed persistent decreases in H3K4me3, H3K27me3 and 5 mC markers in nucleus along with alterations in nuclear size and chromatin compaction percentage in DA-like neurons differentiated from SH-SY5Y cells exposed to 0.4 and 4  $\mu$ g/L PFOA. Among the selected epigenetic features, DNA methylation pattern can be used to distinguish between PFOA-exposed and naïve populations, suggesting the involvement of epigenetic regulation. Moreover, DA-like neurons with pre-differentiation PFOA exposure exhibit altered network connectivity, mitochondrial volume, and TH expression, implying impairment in DA neuron functionality. Collectively, our results revealed the prolonged effects of developmental PFOA exposure on the fitness of DA-like neurons and identified epigenome and mitochondrion as potential targets for bearing long-lasting changes contributing to increased risks of neurological diseases later in life.

### 1. Introduction

Poly- and per-fluoroalkyl substances (PFASs,  $C_nF_{2n+1}$ -R) are a family of highly fluorinated aliphatic compounds with strong acidic, hydrophobic, and lipophobic properties due to the perfluoroalkyl moiety ( $C_nF_{2n+1}$ -) (Chain et al., 2018; Wang et al., 2017), and are used in a wide range of products such as disposable food packaging, cosmetics, aqueous film forming foams, and other consumer products (OECD, 2018). There are more than 4000 types of PFAS (Sunderland et al., 2019), among which perfluorooctanoic acid (PFOA), an organo-fluorine surfactant with a hydrophilic n-octyl head conjugated to a hydrophobic and lipophobic fluorinated carbon tail, is one of the most widely-used (H Nataraj et al., 2015).

Due to the extensive applications of PFOA in different industrial

sectors, PFOA is ubiquitously present in our living environment, including air, soil and water (Paustenbach et al., 2006). The primary route of human exposure to PFOA is via the consumption of contaminated water and food (Garnick et al., 2021). Currently, the US Environmental Protection Agency (EPA) released a health advisory for PFOA in drinking water of 0.07  $\mu$ g/L (EPA, 2016). A recent survey showed that PFOA was detected in drinking water from 33 states in the U.S. with concentrations ranging from 0.02 to 0.35  $\mu$ g/L (Hu et al., 2016). Strikingly, another study shows that the geometric mean of serum PFOA levels for the US population is  $\sim$ 1.42  $\mu$ g/L (CDC, 2021) due to the high stability of PFOA. This number is even higher for people residing at contaminated sites, for example the median serum PFOA concentration measured in mid-Ohio Valley residents were found to be 23.1  $\mu$ g/L (Gallo et al., 2012). PFOA was also detected in umbilical cord sera at 1.6

 $<sup>^{\</sup>star}\,$  This paper has been recommended for acceptance by Dr Jiayin Dai.

<sup>\*</sup> Corresponding author. Davidson School of Chemical Engineering, Purdue University, West Lafayette, IN, 47907, USA. *E-mail address:* cyuan@purdue.edu (C. Yuan).

 $\mu$ g/L (Apelberg et al., 2007), at 0.01–0.05  $\mu$ g/L in breast milk (Zheng et al., 2021), and 8.2  $\mu$ g/L (Mogensen et al., 2015) in infants raising significant concerns about PFOA altering disease risk at a later life following exposures of a development origin of health and disease (DOHaD) paradigm (Gillman, 2005; Haugen et al., 2014).

Several recent studies have suggested neurotoxicity of PFOA. Specifically, zebrafish exposed to 2000 µg/L PFOA for 5 days postfertilization (dpf) showed hyperactive locomotor function at 14 dpf (Jantzen et al., 2016a; Jantzen et al., 2016b). Zebrafish with an embryonic exposure to 1000  $\mu$ g/L PFOA exhibited aberrant locomotor activity, and disruption in dopamine homeostasis (Yu et al., 2021). Furthermore, exposure to PFOA (414-41400 µg/L) can significantly alter neuron activity in a co-culture system of glutamatergic and GABAergic neurons derived from human induced pluripotent stem cells (hiPSCs) by acting as a non-competitive antagonist of human GABAA receptor (Tukker et al., 2020). Altered neuron functions, shown as reduced expression of Tyrosine hydroxylase (TH) and dopamine transporter (DAT), has also been observed in hiPSC-derived dopaminergic (DA) neurons exposed to PFOA of 10 µg/L (Di Nisio et al., 2022). Limited insights, however, were provided regarding cellular targets transmitting the long-lasting damages arising from developmental exposures to

Epigenetic modifications, including DNA methylation, histone posttranslational modifications and RNA processing, are potential molecular markers that can record past-exposure events and transmit diseases to the next generation. The immediate effects of PFOA exposure on epigenome via the regulation of epigenetic enzymes have been reported. For example, reduction of DNA methylation along with dysregulation of TET and DNMT family proteins has been observed in a human liver cell line and murine animal models right after PFOA exposure (Wen et al., 2020a; Wen et al., 2020b). Conversely, N46 (embryonic mouse hypothalamus) cells exposed to PFOA exhibit DNA hypermethylation along with different expressions in DNMTs and TETs (Kim et al., 2021). Epidemiologic studies have shown that prenatal exposure to PFOA caused DNA methylation changes in cord blood of infants at birth (Miura et al., 2018; Kingsley et al., 2017) and suggest a strong correlation between prenatal PFOA exposure with aberrant DNA methylation of children at adolescence (Liu et al., 2022). DNA methylation thus holds the promise as a potential "memory" arising from developmental PFOA exposure.

Bioenergetic adaptation is commonly observed in response to environmental stressors. Mitochondria play a significant role in regulating cellular metabolic bioenergetic levels. Metabolic profiling of a neuronal cell line, SH-SY5Y, showed reductions in ATP-related metabolites and neurotransmitter precursors after exposure to 41400 µg/L PFOA (Souders et al., 2021). Increased mitochondrial reactive oxygen species (ROS) levels and decreased mitochondrial membrane potentials were also observed in the fetus brain of mice after maternal exposure to PFOA of 20 mg/kg (Salimi et al., 2019). Upregulation of lipid synthesis was also observed in the liver of mice treated with PFOA (Weng et al., 2020). Aberrant changes in lipid metabolism induced by PFOA have been postulated to dis-regulate mitochondrial biogenesis and cause changes in mitochondrial structures (Voelker, 2004). These results thus suggest mitochondrial defect as a potential outcome of PFOA exposure.

High PFOA concentrations (10– $414000~\mu g/L$ ) were used in most of past studies, while concentrations relevant to human exposures are significantly lower creating a knowledge gap. Few studies have devised exposure schemes resembling developmental exposures and assessed persistent long-term effects warranting further studies. To address these knowledge gaps, we adopted a model cell line, SH-SY5Y, that is a neural precursor cell (Pezzini et al., 2017; Constantinescu et al., 2007). SH-SY5Y cells can be differentiated into DA-like neurons (Shipley et al., 2016) and thus used for studying developmental exposure effects of various chemicals (Cheung et al., 2009; Lee et al., 2022; Attoff et al., 2020). We exposed SH-SY5Y cells with PFOA before differentiation and examined the effects of PFOA immediately after and till the completion

of differentiation (14 days) to assess persistency.

### 2. Material and methods

# 2.1. Culture and differentiation of SH-SY5Y cells

SH-SY5Y cell lines were obtained from ATCC, seeded into  $\mu\text{-slide}\ 18$  well chambered coverslips (Ibidi) and differentiated using an established protocol (Xie et al., 2021; Lin et al., 2021). Differentiated SH-SY5Y cells become DA-like (Agholme et al., 2010; Borland et al., 2008) and have a high expression of FOXA2, TH and MAP2, which are characteristics of DA-like neurons as shown in Fig. S1 (Supporting Information). Only cells with a passage number lower than 10 were used in our experiments to ensure cellular competency.

PFOA (Sigma Aldrich, Cas # 335-67-1) was dissolved in water at a concentration of 4 mg/L and were spiked into culture medium as described previously (Xie et al., 2021; Lin et al., 2021). SH-SY5Y cells were cultured in PFOA-containing (0.4 or 4  $\mu$ g/L) or free (0  $\mu$ g/L) medium for 4 days. Fresh medium was exchanged every 2 days. Cells were washed with 1  $\times$  PBS three times to remove any residual PFOA before switching to a differentiation medium and cultured for 6 days. Cells were then cultured in a maturation medium for another 8 days to obtain mature DA-like neurons (see Table S1 (Supporting Information) for medium composition). Fresh differentiation and maturation medium were exchanged every 2 days for a total duration of 14 days. The exposure and differentiation paradigm are illustrated in Fig. 1A.

### 2.2. MTT assay

The MTT assay is a colorimetric assay for assessing cell metabolic activity. MTT assay was carried out using a MTT assay kit (Abcam, 211091) following the manufacturer's protocol. After 4 days of PFOA treatment, PFOA-containing medium was removed from culture wells followed by washing in PBS. Cells were then treated with a solution containing 50% serum-free medium and 50% MTT reagents at 37 °C for 3 h, followed by incubation with the MTT solvent at room temperature for 15 min. Absorbance at 580 nm was then collected using a SpectraMax microplate reader (Molecular Device) to determine cell viability.

### 2.3. Fluorescence immuno-staining

Cells were fixed at selected timepoints in 4% formaldehyde (ThermoFisher, USA) at 4 °C overnight and stained as we described previously (Xie et al., 2021; Lin et al., 2021). The primary antibodies used in this study include anti- 5' methyl-cytosine (Active Motif, 61479), H3K4me3 (Abcam, ab8580), H3K27me3 (Abcam, ab192985), TOMM20 (Santa Cruz Biotechnology, sc-17764),  $\alpha$ -synuclein (Invitrogen, 328100), FOXA2 (Invitrogen, A29515), TH (Invitrogen, A29515) and MAP2 (SySy, 188004). Anti-mouse Alexa 568 (Invitrogen, A11004), anti-mouse Alexa 488 (Invitrogen, A11001), anti-rabbit Alexa 568 (Abcam, ab175471) and anti-guinea pig Alexa 647 (Invitrogen, A21450) were used as secondary.

# 2.4. Microscopy imaging

Fluorescence microscopy and DIC images were collected using a high-content imaging platform (ImageXpress Micro Confocal, Molecular Device). DIC images were collected using a Nikon 20  $\times$  /0.75 Plan Apo Lambda objective. Confocal images of cells stained with epigenetic markers and TOMM20 were collected using a Nikon 60  $\times$  /0.95 Plan Apo objective with a z-step interval of 1  $\mu m$ . Confocal images were projected as maximum projections for quantitative analysis. Images of cells stained with TH and MAP2 were collected using a Nikon 20  $\times$  /0.75 Plan Apo Lambda objective.

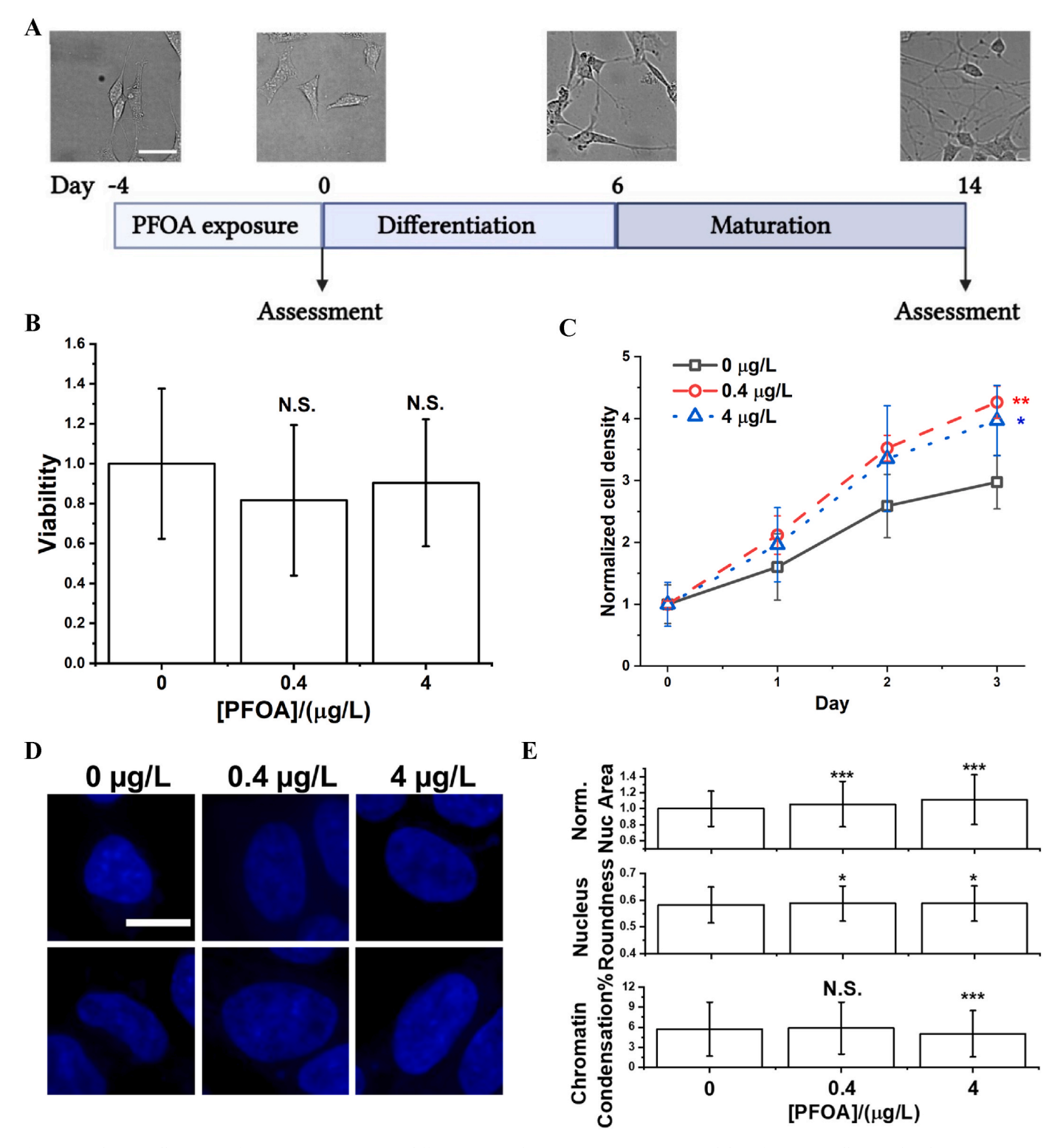


Fig. 1. A) Schematic illustration of PFOA exposure, SH-SY5Y differentiation and assessment timepoints. B) Viability of SH-SY5Y cells treated with 0  $\mu$ g/L, 0.4  $\mu$ g/L and 4  $\mu$ g/L PFOA for 4 days quantified using MTT assay. n=3 independent replicates. C) Growth curve of SH-SY5Y exposed to 0  $\mu$ g/L, 0.4  $\mu$ g/L and 4  $\mu$ g/L PFOA for 3 days. Normalized cell density is calculated using cell area normalized to its corresponding day 0 cell area. n=3 independent replicates. D) Typical images of SH-SY5Y cell nucleus treated with varying concentrations of PFOA. Scale bar = 10  $\mu$ m. E) Bar plots of nucleus morphology, such as nucleus area (top), nucleus roundness (middle) and chromatin condensation percentage (bottom). n>1000 cells from 3 biological replicates. Data = Mean  $\pm$  S.D. N.S.: not significant; \*: p<0.05; \*\*: p<0.01; \*\*\*: p<0.001 (One-Way ANOVA with Tukey post-hoc test).

# 2.5. Image analysis

Neurite morphology analysis was performed via the neurite outgrowth module embedded in MetaXpress Software (Molecular

Device) using DIC images of cells. Nuclear morphology analysis was performed via a customized nuclear segmentation and measurement module through MetaXpress analysis software (Molecular Device) using DAPI stained cells. Chromatin condensation percentage (chromatin

condensation %) was quantified via a Sobel edge detection algorithm described in literature (Irianto et al., 2014). Analysis of single-cell based intensity and foci feature was performed via a CellProfiler Pipeline (Broad Institute) following our established protocol (Xie et al., 2021; Lin et al., 2021). The analysis of mitochondrial volume was carried out using the MiNA plugin of ImageJ via an otsu's auto-threshold method (Valente et al., 2017). All intensity measurements of wide-field fluorescent images were performed on background-corrected images using a Gaussian filter. Intensity of TH on neurites was measured by manually tracing neurite with positive MAP2 staining using the freehand line drawing tool from ImageJ. Traced neurite lines were then expanded to an area with a width of 9 pixels to measure its integrated intensity.

### 2.6. Statistical analysis

We used SH-SY5Y cells from 3 different lineages followed by > 3 independent differentiations. Results of quantitative analysis were reported as mean  $\pm$  standard deviation (S.D.), unless otherwise stated in figure captions. Difference between groups was tested using one-way ANOVA followed by Tukey post-hoc test. p value less than 0.05 was considered significant. All figures along with statistical analysis were prepared using OriginPro (2019). Principal component analysis (PCA) and clustering analysis were performed using prcomp and kmeans function in R (RStudio, v1.2.1).

### 3. Results

### 3.1. Morphological changes in SH-SY5Y cells induced by PFOA treatment

We selected to work with SH-SY5Y cells at a PFOA concentration of 0.4 and 4  $\mu g/L$ . These concentrations were selected based on the serum levels of PFOA from infants at an age of 0–12 months which were found to be 2  $\mu g/L$  at birth and increased to 8.2  $\mu g/L$  at 11 months (Mogensen et al., 2015). We thus used 4  $\mu g/L$  as the higher dose in this study due to its physiological relevance and included 0.4  $\mu g/L$  PFOA due to the prevalence of such concentrations in environment.

To start, we evaluated the toxicity of the selected concentrations of PFOA on cell viability using a MTT assay, with results shown in Fig. 1B. After 96 h of treatment, SH-SY5Y cells did not exhibit significant alterations in cell viability, verifying that the selected PFOA concentrations do not illicit immediate toxicity on treated cells. We also examined the cell growth rate during PFOA exposure as shown in Fig. 1C and observed significantly higher growth rates in PFOA treated cells.

We performed a nuclear morphology analysis on SH-SY5Y cells exposed to 0.4 and 4 µg/L PFOA and compared our findings to the control. Specifically, we fixed the cells after 96 h of exposure and stained cells with DAPI as shown in Fig. 1D and Fig. S2 (Supporting Information). The population mean of nuclear size increased significantly (p < 0.001) by 6 and 11% in 0.4 and 4 µg/L treated SH-SY5Y cells (see Fig. 1E top panel). Changes in nuclear shape were also observed suggesting a rounder nuclear morphology after PFOA treatments (see Fig. 1E middle panel). Changes in nuclear size and shape is often associated with alterations in chromatin compaction. Therefore, we performed chromatin condensation analysis following an established protocol (Irianto et al., 2014). We observed a significant decrease ( $\sim$ 12%, p < 0.001) of chromatin condensation percentage in cells treated with 4 µg/L PFOA (Fig. 1E bottom panel). No significant changes were found in cells exposed to 0.4 µg/L PFOA.

# 3.2. Morphological changes in DA-like neurons differentiated from SH-SY5Y after a developmental-like PFOA exposure

To demonstrate the prolonged effect of developmental PFOA exposure on neurons, the treated cells were differentiated into DA-like neurons following a 14-day differentiation protocol using PFOA-free medium as we described previously (Xie et al., 2021; Lin et al., 2021)

(see also Fig. 1A). The formation of DA-like neurons was verified via FOXA2, TH and MAP2 staining as shown in Fig. S1 (Supporting Information). Specifically, undifferentiated SH-SY5Y has low levels of FOXA2. The expression of FOXA2, a transcriptional factor for DA neuron maintenance, was significantly elevated in differentiated SH-SY5Y cells (Day 14). A similar trend was observed for MAP2 and TH verifying the DA-like characteristics in differentiated SH-SY5Y cells.

Morphological assessments, including nuclear conformation and chromatin condensation %, were carried out similarly as described in the previous section. Additionally, we analyzed the neuron network by focusing on changes in process numbers, neurite length and branch numbers. Typical images of DAPI stained neurons are shown in Fig. 2A and Fig. S3A (Supporting Information). Among them, significant increases in nucleus size were observed in cells treated with 0.4  $\mu$ g/L (~1%, p < 0.001) and 4  $\mu$ g/L (~3%, p < 0.001) PFOA (see Fig. 2B top panel), a trend persistent with what was observed prior to differentiation but at a reduced level. No significant change was observed in nucleus roundness (Fig. 2B middle panel). Chromatin condensation percentage increased significantly (~5%, p < 0.001) in 0.4  $\mu$ g/L PFOA treated cells, while decreased significantly (~4%, p < 0.05) in 4  $\mu$ g/L PFOA treated cells (Fig. 2B bottom panel).

Analysis of neuron network revealed significant reductions in complexity arising from PFOA exposure as shown in Fig. 2C and Fig. S3B (Supporting Information). Specifically, the number of neurite branches decreased significantly by  $\sim\!11\%$  and 13% for neurons treated with 0.4 and 4 µg/L PFOA (see Fig. 2D top panel). No significant changes were found in neurite length (see Fig. 2D middle panel). Significant decrease in process numbers (axon number from each soma body) was also observed in neurons exposed to 4 µg/L PFOA, but not in those exposed to 0.4 µg/L PFOA (see Fig. 2D bottom panel).

### 3.3. Epigenetic changes in SH-SY5Y cells induced by PFOA exposure

Given the significant changes in nuclear morphology and chromatin condensation percentage after PFOA exposure, we further investigated changes in the epigenome in response to PFOA treatment. SH-SY5Y cells were fixed immediately after 96 h of PFOA exposure and stained for H3K4me3, H3K27me3 and 5 mC, as shown in Fig. 3A-C and Fig. S4A-S4C (Supporting Information). SH-SY5Y cells exhibited diffusive patterns of H3K4me3 inside cell nucleus with mild enrichment as small puncta. Global abundance of H3K4me3 decreased modestly in  $0.4 \mu g/L$ (~9%, p < 0.001) and 4  $\mu$ g/L (~3%, p < 0.01) PFOA treated cells as shown in Fig. 3D. Spatial distribution and puncta-like features of H3K4me3 were further quantified using CellProfiler following published protocols (Xie et al., 2021; Lin et al., 2021). Multi-dimensional data extracted from immunostaining pattern was then plotted on a principal component (PC) space to identify possible new subpopulations arising from PFOA treatment. No distinct separation among varying doses was identified from H3K4me3 staining (Fig. 3G).

H3K27me3 staining shows punctate patterns with one large foci, also known as Barr body, in each nucleus (Fig. 3B and Fig. S4B (Supporting Information)). Intensity analysis showed  $\sim\!12\%~(p<0.001)$  decrease of H3K27me3 in 0.4 µg/L PFOA treated cells, while  $\sim\!6\%~(p<0.001)$  decrease was observed in 4 µg/L PFOA treated cells (see also Fig. 3E). Principal component analysis (PCA) plot (see Fig. 3H) shows no distinctive separations between PFOA exposed and untreated cells.

We also examined changes of DNA methylation in response to PFOA exposure using 5 mC staining. 5 mC staining showed a punctate pattern inside cell nucleus with significant enrichment on nuclear periphery (Fig. 3C and Fig. S4C (Supporting Information)), as expected for heterochromatin markers. Total intensity analysis (Fig. 3F) showed a dramatic decrease of 5 mC in PFOA exposed cells. Specifically, 5 mC decreased by  $\sim\!27\%$  (p<0.001) in 0.4 µg/L PFOA exposed cells and  $\sim\!19\%$  (p<0.001) in 4 µg/L PFOA exposed cells. The PCA plot of 5 mC patterns showed a distinctive separation between PFOA treated and unexposed cells. To further validate the separations visualized in the

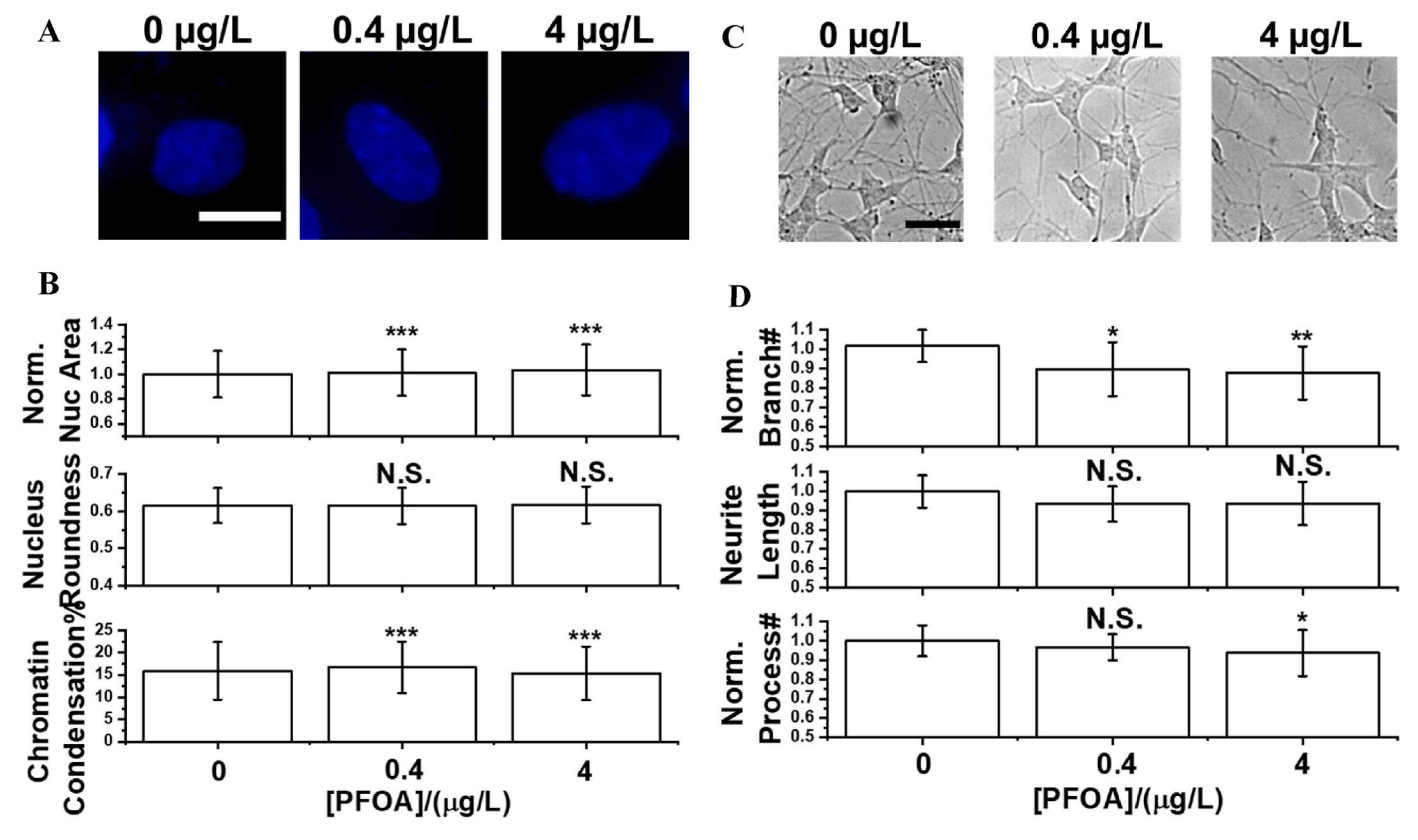


Fig. 2. A) Representative images of differentiated SH-SY5Y stained with DAPI. Scale bar =  $10 \mu m$ . B) Bar plots of nucleus morphology, including nucleus area, nucleus roundness and chromatin condensation percentage (from top to bottom). n > 1000 cells from 3 biological replicates. C) Representative DIC images of differentiated SH-SY5Y cells. Scale bar =  $50 \mu m$ . D) Bar plots of neuron morphology parameters, including branch number, neurite length and process (from top to bottom). n > 16 independent replicates. Data = Mean  $\pm$  S.D. N.S.: not significant; \*: p < 0.05; \*\*: p < 0.01; \*\*\*: p < 0.001 (One-Way ANOVA with Tukey posthoc test).

PCA plot, *k*-means clustering analysis was performed to define subpopulations, shown as grey circles in Fig. 3I. The percentage of cells from PFOA treatment group in each cluster was also quantified as shown in Fig. S5A (Supporting Information). Specifically, cluster 1 was dominated by unexposed cells, while cluster 2 was dominated by 0.4 and 4 µg/L PFOA exposed cells. Cluster 3 was a mixture of all PFOA treatment groups. Least absolute shrinkage and selection operator (LASSO) analysis was also performed to distinguish parameters contributing most to the separation of subpopulations as shown in Table S2 (Supporting Tables). Our results showed that intensity- and foci-texture-based features of 5 mC are major contributors to distinguish between differently treated SH-SY5Y cells.

### 3.4. Epigenetic changes in differentiated SH-SY5Y cells induced by predifferentiation PFOA treatment

A similar analysis was performed with differentiated SH-SY5Y cells stained for H3K4me3, H3K27me3 and 5 mC as summarized in Fig. 4A–C and Fig. S6A-6C (Supporting Information). DA-like neurons differentiated from SH-SY5Y with a pre-differentiation exposure to PFOA show diffusive patterns of H3K4me3 with enrichment near nucleolus, as shown in Fig. 4A and Fig. S6A (Supporting Information). Integrated intensity of H3K4me3 decreased by  $\sim\!6\%~(p<0.001)$  in 0.4 µg/L PFOA treated cells.  $\sim9\%~(p<0.001)$  decrease of total H3K4me3 was observed in 4 µg/L PFOA treated cells (Fig. 4D). H3K4me3 pattern was not distinguishable between PFOA treated and untreated group from the PCA plot as shown in Fig. 4G.

H3K27me3 staining of differentiated SH-SY5Y cells showed punctate patterns as expected (see Fig.4B and Fig. S6B (Supporting Information)). H3K27me3 level decreased by  $\sim\!17\%~(p<0.001)$  in 0.4  $\mu\mathrm{g}/\mathrm{L}$  PFOA

treated cells and  $\sim 10\%$  (p < 0.001) in 4 µg/L PFOA treated cells as shown in Fig. 4E. The PCA plot based on H3K27me3 staining does not show distinct separations between PFOA treated and untreated cells (Fig. 4H).

Neurons showed small foci-like features for 5 mC inside nucleus with a significant enrichment near nuclear periphery as shown in Fig. 4C and Fig. S6C (Supporting Information). 5 mC level decreased dramatically in the PFOA treated group (see Fig. 4F). Notably, we observed ~37% decrease (p < 0.001) in 0.4  $\mu$ g/L PFOA treated group and ~58% decrease (p < 0.001) in 4  $\mu$ g/L PFOA treated group, respectively. The PCA plot based on 5 mC patterns shows distinctive separations. Specifically, the PFOA treated group gradually shifted away from the untreated group with increasing doses as shown in Fig. 4I. Clustering analysis showed that 0 µg/L PFOA treated cells formed a cluster with minimal overlap with 0.4  $\mu$ g/L and 4  $\mu$ g/L PFOA treated cells. 0.4  $\mu$ g/L PFOA treated cells formed a new cluster with some overlap with 4 µg/L PFOA treated cells. A subpopulation of  $4 \mu g/L$  treated cells formed a new distinctive cluster. This observation was further validated by quantifying the percentage of cells in each cluster (see Fig. S5B (Supplementary Information)). Cluster 1 is dominated by unexposed cells. Cluster 2 is dominated by  $0.4~\mu g/L$  PFOA exposed cells. Cluster 3 is shared between 0.4 µg/L and 4 µg/L PFOA exposed cells. Top 2 features ranked with LASSO coefficient were texture-based features, as shown in Table S3 (Supporting Information).

### 3.5. Changes in mitochondrial morphology induced by PFOA exposure

To elucidate the impact of PFOA exposure on cell bioenergetics, we measured mitochondrial volume right after PFOA exposure and after the completion of differentiation. SH-SY5Y cells were exposed to  $0.4~\mu g/L$ 

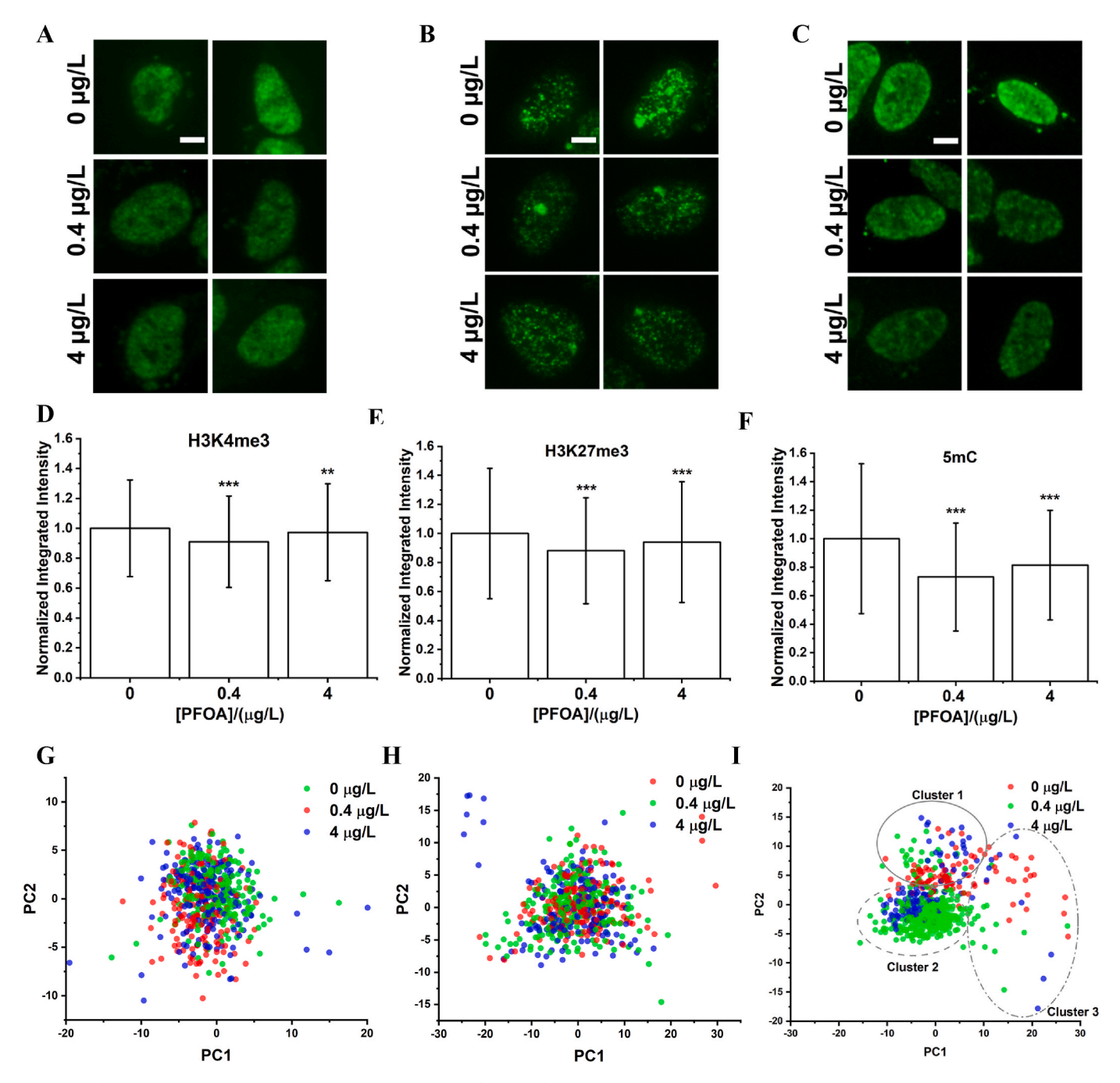


Fig. 3. Pre-differentiation. A-C) Representative images of SH-SY5Ycells exposed to 0  $\mu$ g/L, 0.4  $\mu$ g/L and 4  $\mu$ g/L of PFOA stained for A) H3K4me3, B) H3K27me3 and C) 5 mC prior to differentiation. Scale bar = 5  $\mu$ m. D-F) Normalized integrated intensity from single cells stained with D) H3K4me3, E) H3K27me3 and F) 5 mC n > 1000 cells from 3 different passages. G-I) PCA plots of single cell features extracted from G) H3K4me3, H) H3K27me3 and I) 5 mC staining of SH-SY5Y treated with various doses of PFOA. PCA space was constructed using >1000 cells per condition, 600 cells were randomly selected from each group and included in the PCA plots. \*\*: p < 0.001 (One-way ANOVA with Tukey post-hoc test).

and 4  $\mu$ g/L PFOA for 96 h and stained for TOMM20 as shown in Fig. 5A and Fig. S7A (Supporting Information). Mitochondria showed a polarized distribution in cytoplasm of unexposed SH-SY5Y cells. Cells treated with 0.4 and 4  $\mu$ g/L PFOA, however, have a more uniform distribution of mitochondria around nucleus. Elongated and connected mitochondria structure was observed along the polarized axis of the cell in the untreated control. No such structure was observed in 0.4 and 4  $\mu$ g/L PFOA treated cells, where mitochondria showed more fragmented structures as shown in the zoom-in views in Fig. 5A and Fig. S7A (Supporting Information). The total volume of mitochondria in each cell was quantified via MiNA plugin in ImageJ, normalized to the untreated group and

summarized in Fig. 5B. We observed no significant changes in mito-chondrial volume right after PFOA exposure.

We performed a similar analysis of mitochondrial morphology and volume using DA-like neurons differentiated from SH-SY5Y cells exposed to PFOA. Mitochondria in neurons are highly polarized and are enriched near the soma as shown in Fig. 5C and Fig. S7B (Supporting Information). Mitochondrial morphology is more condensed in 0.4 and 4 ppb (µg/L) PFOA treated cells. Mitochondrial volume decreased by  $\sim\!\!35\%$  (p<0.001) in 0.4 µg/L PFOA treated cells; and by  $\sim\!\!38\%$  (p<0.001) in 4 µg/L PFOA treated cells compared to the untreated cells (see Fig. 5D).

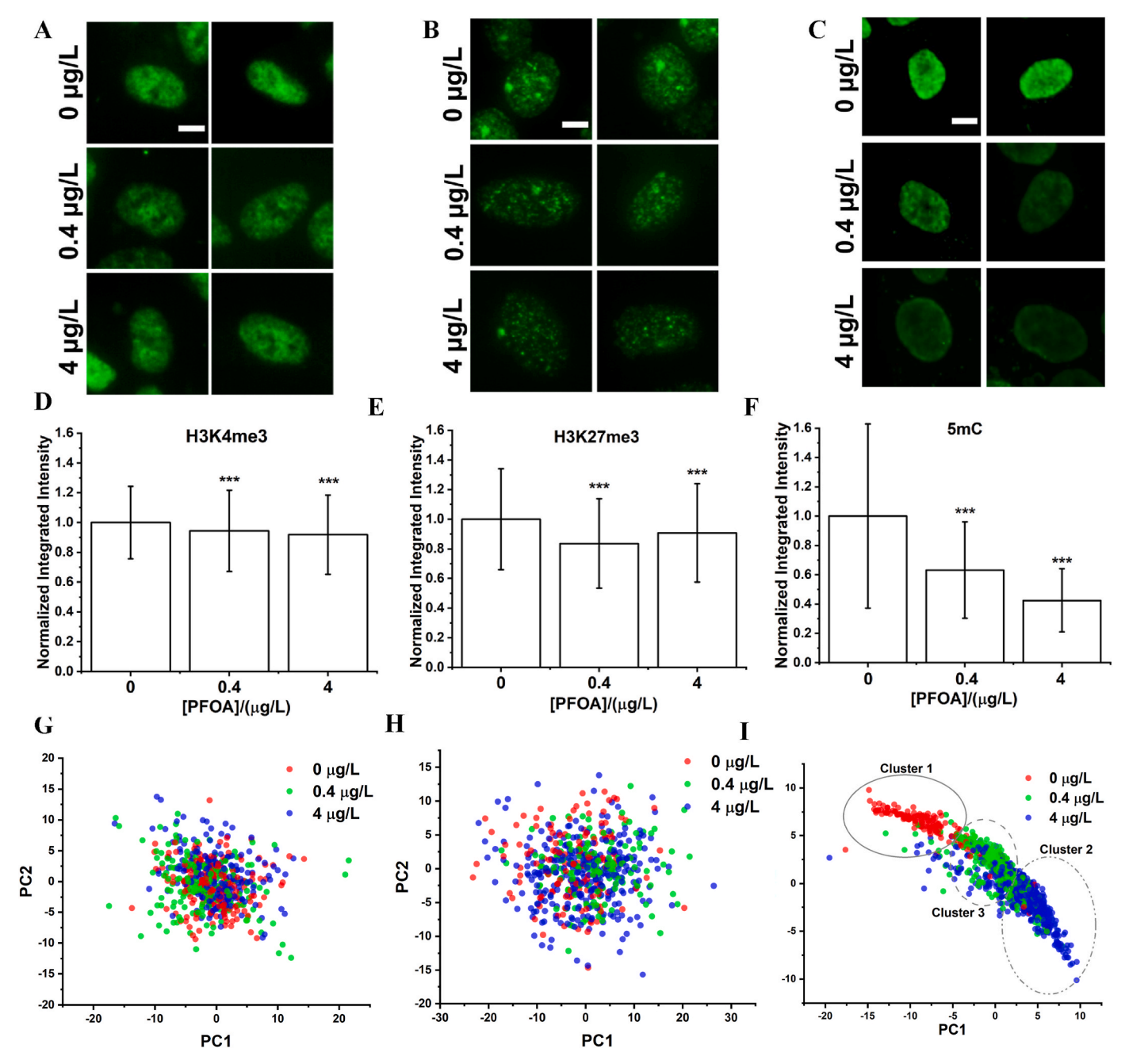


Fig. 4. Post-differentiation. A-C) Representative images of SH-SY5Y cells exposed to 0  $\mu$ g/L, 0.4  $\mu$ g/L and 4  $\mu$ g/L, differentiated and then stained for A) H3K4me3, B) H3K27me3 and C) 5 mC Scale bar = 5  $\mu$ m. D-F) Normalized integrated intensity from single cell stained with D) H3K4me3, E) H3K27me3 and F) 5 mC n > 1000 cells from 3 independent differentiation. G-I) PCA plot of single cell features extracted from G) H3K4me3, H) H3K27me3 and I) 5 mC staining of differentiated SH-SY5Y. PCA space was constructed using >1000 cells per conditions, 600 cells were randomly selected from each group and included in the PCA plots. \*\*\*: p < 0.001 (Oneway ANOVA with Tukey post-hoc test).

### 3.6. Changes in DA-neuron characteristics induced by PFOA exposure

DA-like neurons are unique in their abilities to form synapses, release dopamine and enable synaptic communications. We thus assessed the expression levels of TH and SNCA in the DA-like neurons differentiated from SH-SY5Y.

DA-like neurons differentiated from PFOA-exposed and naïve SH-SY5Y cells all showed positive TH staining in both soma body and neurites as shown in Fig. 6A and Fig. S8A (Supporting Information). The total intensity of TH per cell was quantified and normalized to the untreated control as shown in Fig. 6B. The TH intensity per cell showed  $\sim\!29\%~(p<0.001)$  decrease in 0.4 µg/L PFOA treated neurons and

 ${\sim}32\%~(p<0.001)$  decrease in 4 µg/L PFOA treated neurons. TH is normally enriched near synaptic junctions, and we thus quantified TH levels in neurites, marked by MAP2, a commonly used neuronal cytoskeleton marker as shown in Fig. 6C and Fig. S8B (Supporting Information). We quantified TH intensity along neurite and normalized to the untreated control as shown in Fig. 6D. TH intensity on neurites decreased by  ${\sim}14\%~(p<0.001)$  in 0.4 µg/L PFOA treated neurons; and  ${\sim}13\%~(p<0.001)$  in 4 µg/L PFOA treated neurons.

SNCA staining showed enrichments near soma body and neurites as shown in Fig. S9A (Supporting Information). The average SNCA expression per cell was quantified, normalized to the untreated sample and showed mild decreases ( $\sim$ 5%, p < 0.05) only in 4 µg/L PFOA treated

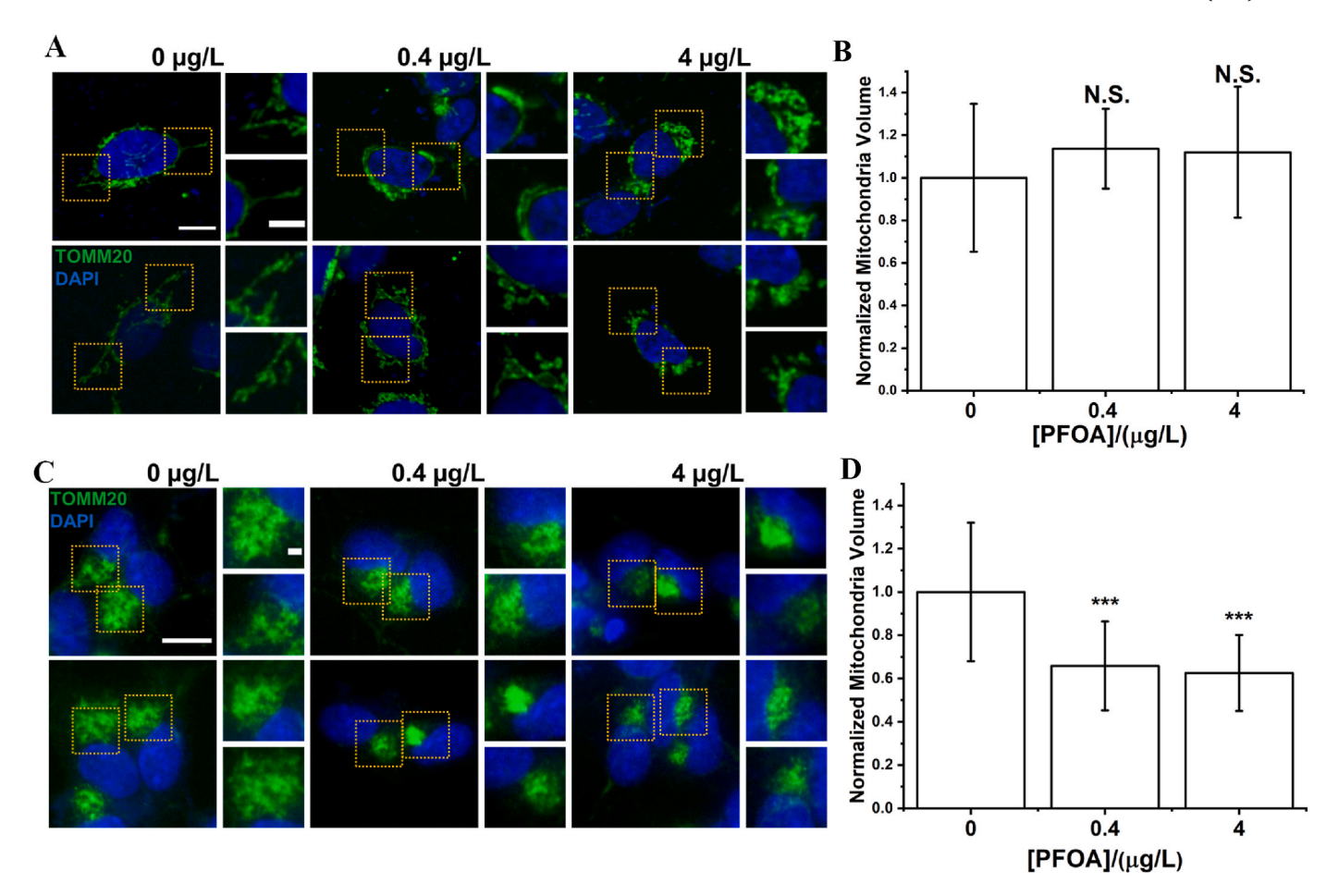


Fig. 5. A) Representative images of SH-SY5Y cells after exposed to 0  $\mu$ g/L, 0.4  $\mu$ g/L and 4  $\mu$ g/L PFOA stained for TOMM20. Scale bar = 10  $\mu$ m for whole-cell images. Scale bar = 2  $\mu$ m for zoom-in images. B) Volume analysis of TOMM20 staining of pre-differentiation SH-SY5Y. C) Representative images of differentiated SH-SY5Y cells with pre-differentiation exposure to 0  $\mu$ g/L, 0.4  $\mu$ g/L and 4  $\mu$ g/L PFOA stained with TOMM20. Scale bar = 10  $\mu$ m for whole-cell images. Scale bar = 2  $\mu$ m for zoom-in images. D) Volume analysis of TOMM20 staining of differentiated SH-SY5Y.  $n \ge 20$  cells from three independent differentiations. N.S.: not significant; \*\*\*: p < 0.001(One-way ANOVA with Tukey post-hoc test).

cells as shown in Fig. S9B (Supporting Information).

# 4. Discussions

We selected SH-SY5Y cells to assess neurotoxicity mimicking a developmental exposure. SH-SY5Y cell is a human cell line derived from a neuroblastoma patient and is uniquely capable of differentiating into DA like neurons. SH-SY5Y cells are commonly accepted as neuronal precursors with the ability to differentiate into DA neurons (Pezzini et al., 2017; Constantinescu et al., 2007). Differentiated SH-SY5Y cells showed DA neuron like characteristics, which have been validated via transcriptional profiling (Korecka et al., 2013), immuno-histology analysis (Cheung et al., 2009; Lopes et al., 2012), and dopamine uptake assays (Mastroeni et al., 2009). SH-SY5Y has thus been widely adopted as a viable model for neurotoxicity particularly for Parkinson's disease (PD). For example, SH-SY5Y can recapitulate PD related phenotypes such as synuclein aggregation after exposure to rotenone (Borland et al., 2008). Here we used SH-SY5Y cells to mimic neural progenitor cells that have already committed to a specific lineage but retain the ability to replicate. Neural progenitor cells exist in fetal brains during the whole gestational stage (Yin et al., 2013). Therefore, we exposed undifferentiated SH-SY5Y cells to PFOA to mimic a developmental exposure, removed PFOA, initiated neuron differentiation and assessed changes in mature neurons (Day 14) to study long-term persisting effects of PFOA on neurons.

SH-SY5Y cells exhibit significant alterations in nuclear morphology

immediately after PFOA exposure and the changes partially prevail after the cessation of exposure and the completion of differentiation. Many factors can contribute to alterations in nuclear morphology, including cell cycles (Fidorra et al., 1981; Schooley et al., 2012; Roca-Cusachs et al., 2008), chromatin compactness (Stephens et al., 2018; Wang et al., 2018) and cellular stress (Panagaki et al., 2021; Shah et al., 2021). Prior to differentiation, SH-SY5Y cells were still actively proliferating with accelerated growth in PFOA-exposed cells. Increased growth rate induced by low dose PFOA exposure was previously observed in several cell lines and animal models. For example, increased proliferation was observed in preadipocytes exposed to 10-100000 µg/L PFOA (Ma et al., 2018). Human breast epithelial cells (MCF-10A) showed significantly higher growth rate after exposure to 20700 µg/L PFOA (Pierozan et al., 2018). PFOA was shown to upregulate Cyclin D and CDK4 which promote G1/S phase transition and subsequently cellular growth in both human breast cancer (Pierozan et al., 2018; Pierozan et al., 2020) and granulosa cell line (Clark et al., 2022). A similar mechanism may also contribute to the increased growth rate of SH-SY5Y. Cells during S phase have expanded nuclear sizes when compared to those at interphases (Roca-Cusachs et al., 2008). Our observations, that PFOA exposed cells showed larger nuclear size, can thus be partially explained by the accelerated proliferations of PFOA-exposed SH-SY5Y cells, which is consistent with prior literature suggesting that PFOA can accelerate the transition between G1/G0 to S phase and increase cell growth rates (Pierozan et al., 2018; Pierozan et al., 2020). Chromatin condensation can also contribute to the observed changes in nuclear morphology. The

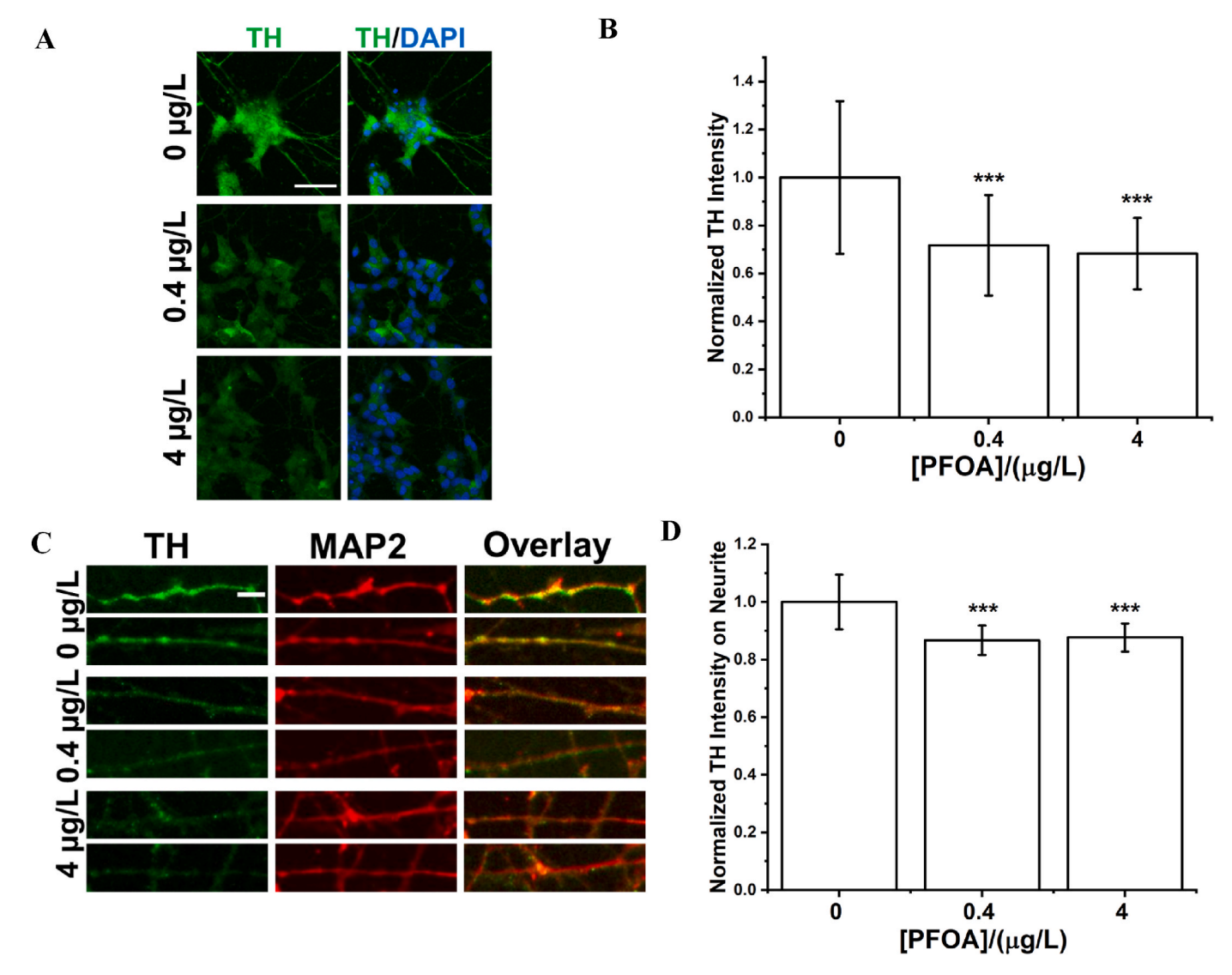


Fig. 6. A) Representative images of differentiated SH-SY5Y cells stained for TH and DAPI. Scale bar =  $50 \mu m$ . B) Total intensity of TH normalized by cell number. n > 50 sites from 3 independent differentiations. C) Representative images of differentiated SH-SY5Y cell neurites stained for TH and MAP2. Scale bar =  $10 \mu m$ . D) Intensity of TH per neurite length (intensity/pixel) normalized to the untreated control.  $n \ge 30 \text{ cells}$ . \*\*\*: p < 0.001 (One-way ANOVA with Tukey post-hoc test).

chromatin of PFOA exposed cells is less compact which may also contribute to the observed increases in nuclear size right after PFOA exposure. Changes in nuclear size diminish after the completion of differentiation but remain significant. These changes potentially arise from persistent alterations in chromatin compaction and imply impairments in differentiated DA-like neurons. Abnormal nuclear morphology are commonly observed in various disease models, including cancers and neurodegenerative diseases (Frost, 2016). For example, the nuclear size of rostral midbrain neurons were found to be significantly bigger in patients with Parkinson's disease (PD) compared to the healthy control (Colpan and Slavin, 2010). Increased nuclear size was also observed in mouse DA neurons carrying LRRK2 mutation, a genetic risk factor of PD (Tsika et al., 2014).

Chromatin compactness is regulated by epigenetic modifications, encoded by an array of histone modifications. We selected three modifications here, including bivalent markers (H3K4me3 and H3K27me3) and a suppressive marker (5 mC) due to their critical roles in determining differentiation lineages (Bernstein et al., 2006; Sachs et al., 2013) and neurological disorders (Jin and Liu, 2018). We observed reductions in all three selected markers immediately after PFOA exposure and the decreases persist after the completion of neuron differentiation.

Among them, the decrease in 5 mC further attenuates. Our results also suggest that intensity- and foci-texture-based features of 5 mC are major contributors to distinguish between differently treated SH-SY5Y cells. This trend partially aligns with our observations in chromatin condensation % which suggests that PFOA induces the formation of less compact chromatin potentially arising from the loss of bivalent and repressive epigenetic markers. Similar trends were observed in cancer cell lines, including MCF7 and HepG2 which exhibit loss in both DNA methylation and histone methylation, for example H3K9me3, after exposure to  $> 40000 \,\mu\text{g/L}$  PFOA (Wen et al., 2020a; Liu and Irudayaraj, 2020). Consistent changes were also observed in various cell and tissues following PFOA exposure, including preadipocytes (Ma et al., 2018), mouse kidney (Rashid et al., 2020), liver cancer cell line (Wen et al., 2020a) and human breast cell line (Pierozan et al., 2020). Less, however, is known about changes in bivalent markers, such as H3K4me3 and H3K27me3, after PFOA exposure. MCF10A cells did not show significant changes in H3K4me3 right after exposure but were manifested in daughter cells after exposing to 41407 µg/L PFOA (Pierozan et al., 2020). Mouse oocytes exposed to high doses of PFDA, a chemical belonging to the same PFAS family and with a similar structure to PFOA, showed decreases in global H3K4me3 levels (Deng et al., 2021).

Similarly, mouse embryonic stem cells exposed to high doses of PFOS (>10000  $\mu$ g/L) can alter the expression of EZH2, a H3K27me3 methyltransferase, and ultimately change the expression of pluripotent genes (Xu et al., 2015).

No studies, however, have assessed the persistency of chromatin and epigenetic changes in neurons after the cessation of developmental PFOA exposure to the best of our knowledge. Our data has unequivocally revealed the establishment of a persistently altered chromatin state featuring less repressive epigenetic markers and more permissive chromatins after PFOA exposure.

DNA methylation patterns, instead of intensity, can serve as good classifiers distinguishing among SH-SY5Y cells exposed to various doses of PFOA. The distinction is more obvious for SH-SY5Y cells post-differentiation compared to those cells assessed immediately after exposure suggesting DNA methylation as a potential regulator governing the transition in chromatin states. The PFOA exposure effects, however, do not necessarily follow a linear dose dependence. Conversely, changes in selected epigenetic markers, including DNA methylation, are seemingly more significant for PFOA at 0.4  $\mu g/L$  compared to 4  $\mu g/L$  after exposure and prior to differentiation.

After differentiation, neurons exposed to the higher dose of PFOA (4 µg/L) have larger changes than those exposed to the lower concentration (0.4 µg/L). Cells adapt to environmental exposures by altering transcriptomic and metabolic profiles. Cellular adaptation mechanism can lead to over-compensation (Goyal et al., 2019) and thus plausibly account for the difference in dose-dependence as we observed in this work before and after differentiation. It is interesting to note that abnormal changes in bivalent epigenetic markers and 5 mC are also common features in neurogenerative diseases. For example, the loss of Polycomb repressive complex 2 (PRC2), which catalyzes H3K27 trimethylation, promotes neuron death and facilitates neurodegeneration (von Schimmelmann et al., 2016). Loss of H3K4me3 was also observed in Huntington disease, where reducing the expression of H3K4me3 demethylase are found to be neuroprotective in a mouse model (Vashishtha et al., 2013). Decreased levels of H3K27me3 and H3K4me3 were observed in SH-SY5Y cells treated with 6-OHDA, a commonly used neurotoxin to induce PD phenotype (Mu et al., 2020). DNA hypomethylation of TNF $\alpha$  was observed in the substantia nigra of PD patients (Pieper et al., 2008). Hypomethylation of CpH sites in enhancers was also found in the prefrontal cortex neurons from patients with Alzheimer's disease (Li et al., 2019).

The collective results have thus led us to postulate functional alterations in DA-like neurons and PFOA as a developmental neurotoxin. The differentiated SH-SY5Y cells exhibit characteristic features of DA neurons with and without PFOA exposure. The neurite network, however, has decreased levels of complexity with smaller process and branch numbers. Reductions in SNCA expression, a protein mediating the clustering of synaptic vesicles (Diao et al., 2013), were also observed suggesting the potential loss of synaptic activities and signal strengths. Furthermore, the expression of TH was also decreased in differentiated SH-SY5Y cells implying reductions in dopamine productions. The maintenance of neuron functions is extremely energy demanding. Mitochondrion as a bioenergetic center is thus critically important. Although no significant changes were observed in mitochondrial volume right after exposure, differentiated SH-SY5Y cells have smaller volume of mitochondria. PFOA can bind to peroxisome proliferator activated receptors (PPARs), cause developmental defects (Wolf et al., 2008; Abbott et al., 2012; Abbott et al., 2007; Almeida et al., 2021), and thus a target of PFOA toxicity. PPARs modulate fatty acid oxidation and regulate mitochondrial biogenesis (Oka et al., 2011; Miglio et al., 2009; Ghosh et al., 2007). Furthermore, PFOA can also alter the synthesis and metabolism of lipids (Yu et al., 2016) and was shown to induce abnormality in autophagosomes (Weng et al., 2020). Collectively, changes in PPAR and lipid contents may contribute to the observed alterations in mitochondrial morphology and volume.

Taken together, the changes in molecular markers, including

neurites, TH, SNCA and mitochondrion, suggest altered neuron activities after PFOA exposures and share remarkable resemblance to the characteristics commonly observed in neurodegenerative disease models, particularly PD. For example, overexpression of SNCA mutant, a well-known genetic risk of PD, induced decreased neurite outgrowth and neurite branching in midbrain neurons of rats (Koch et al., 2015). Decreased transcription of SNCA was observed in substantia nigra neurons in PD patients showing Lewy body formation (Kingsbury et al., 2004; Neystat et al., 1999; Su et al., 2017). Loss of TH expression has also been widely observed in substantia nigra neurons in PD brains (Javoy-Agid et al., 1990) and neurons exposed to exogenous PD risk factors, such as MPTP (Alam et al., 2017; Kozina et al., 2014). Mitochondria dysfunction has long been considered as a hallmark of PD, pioneered by a study that associated mitochondria complex I activity with PD (Schapira et al., 1990). Mutations on PINK1 and Parkin, two genetic risk factors of familiar PD, play a significant role in mitophagy and regulates mitochondrial maintenance (Narendra et al., 2010). Decrease of mitochondrial volume was also observed in DA neurons of mice with Drp1 knockout, which is correlated with midbrain neurodegeneration (Berthet et al., 2014).

### 5. Conclusions

Low-dose exposure of PFOA during a pre-differentiation window can induce persistent changes in nuclear morphology and selected epigenetic markers, including H3K4me3, H3K27me3 and 5 mC, at a neuronal lineage. DA-like neurons derived from PFOA-exposed SH-SY5Y cells exhibit abnormal SNCA and TH expression, aberrant mitochondrial volume, and reduced network complexity aligning with a neurodegenerative disease phenotype. Collectively, our results suggest that low dose exposure to PFOA prior to terminal neuron differentiation can cause long-lasting damages in neurons and PFOA as a potential neurotoxin.

# **CRediT** author statement

- **H. Zhao:** Experiment, Data Curation and Analysis, Visulaization and Analysis, Writing- Reviewing and Editing.
  - J. Xie: Data Analysis, Methodology, Experiment and Reviewing.
  - S. Wu: Data Analysis, Reviewing and Editing.
  - O. Sanchez: Writing, and Reviewing.
  - X. Zhang: Experiment.
  - J. Freeman: Conceptualization, Reviewing and Supervising.
- $\mbox{\bf C. Yuan:}$  Conceptualization, Methodology, Writing- Reviewing, Editing and Supervising.

# Declaration of competing interest

The authors declare that they have no known competing financial interests or personal relationships that could have appeared to influence the work reported in this paper.

### Data availability

Data will be made available on request.

### Acknowledgments

This work was supported by National Science Foundation [CBET-1705560 & EF-1935226].

### Appendix A. Supplementary data

Supplementary data to this article can be found online at https://doi.org/10.1016/j.envpol.2022.119684.

#### References

- Abbott, B.D., Wolf, C.J., Schmid, J.E., Das, K.P., Zehr, R.D., Helfant, L., Nakayama, S., Lindstrom, A.B., Strynar, M.J., Lau, C., 2007. Perfluorooctanoic acid-induced developmental toxicity in the mouse is dependent on expression of peroxisome proliferator-activated receptor-alpha. Toxicol. Sci. 98 (2), 571–581.
- Abbott, B.D., Wood, C.R., Watkins, A.M., Tatum-Gibbs, K., Das, K.P., Lau, C., 2012. Effects of perfluorooctanoic acid (PFOA) on expression of peroxisome proliferator-activated receptors (PPAR) and nuclear receptor-regulated genes in fetal and postnatal CD-1 mouse tissues. Reprod. Toxicol. 33 (4), 491–505.
- Agholme, L., Lindström, T., Kågedal, K., Marcusson, J., Hallbeck, M., 2010. An in vitro model for neuroscience: differentiation of SH-SY5Y cells into cells with morphological and biochemical characteristics of mature neurons. J. Alzheim. Dis. 20, 1069–1082.
- Alam, G., Edler, M., Burchfield, S., Richardson, J.R., 2017. Single low doses of MPTP decrease tyrosine hydroxylase expression in the absence of overt neuron loss. Neurotoxicology 60, 99–106.
- Almeida, N.M.S., Eken, Y., Wilson, A.K., 2021. Binding of per- and polyfluoro-alkyl substances to peroxisome proliferator-activated receptor gamma. ACS Omega 6 (23), 15103–15114
- Apelberg, B.J., Goldman, L.R., Calafat, A.M., Herbstman, J.B., Kuklenyik, Z., Heidler, J., Needham, L.L., Halden, R.U., Witter, F.R., 2007. Determinants of fetal exposure to polyfluoroalkyl compounds in baltimore, Maryland. Environ. Sci. Technol. 41 (11), 3891–3897.
- Attoff, K., Johansson, Y., Cediel-Ulloa, A., Lundqvist, J., Gupta, R., Caiment, F., Gliga, A., Forsby, A., 2020. Acrylamide alters CREB and retinoic acid signalling pathways during differentiation of the human neuroblastoma SH-SY5Y cell line. Sci. Rep. 10 (1), 16714.
- Bernstein, B.E., Mikkelsen, T.S., Xie, X., Kamal, M., Huebert, D.J., Cuff, J., Fry, B., Meissner, A., Wernig, M., Plath, K., Jaenisch, R., Wagschal, A., Feil, R., Schreiber, S. L., Lander, E.S., 2006. A bivalent chromatin structure marks key developmental genes in embryonic stem cells. Cell 125 (2), 315–326.
- Berthet, A., Margolis, E.B., Zhang, J., Hsieh, I., Zhang, J., Hnasko, T.S., Ahmad, J., Edwards, R.H., Sesaki, H., Huang, E.J., Nakamura, K., 2014. Loss of mitochondrial fission depletes axonal mitochondria in midbrain dopamine neurons. J. Neurosci. 34 (43), 14304.
- Borland, M.K., Trimmer, P.A., Rubinstein, J.D., Keeney, P.M., Mohanakumar, K.P., Liu, L., Bennett, J.P., 2008. Chronic, low-dose rotenone reproduces Lewy neurites found in early stages of Parkinson's disease, reduces mitochondrial movement and slowly kills differentiated SH-SY5Y neural cells. Mol. Neurodegener. 3 (1), 21.
- CDC, 2021. Fourth national report on human exposure to environmental chemicals, updated tables, march 2021. In: Volume One, Services, U. S. D. O. H. a. H..
- Chain, E. P. o. C. i. t. F., Knutsen, H.K., Alexander, J., Barregård, L., Bignami, M., Brüschweiler, B., Ceccatelli, S., Cottrill, B., Dinovi, M., Edler, L., 2018. Risk to human health related to the presence of perfluorooctane sulfonic acid and perfluorooctanoic acid in food. EFSA J. 16 (12), e05194.
- Cheung, Y.-T., Lau, W.K.-W., Yu, M.-S., Lai, C.S.-W., Yeung, S.-C., So, K.-F., Chang, R.C.-C., 2009. Effects of all-trans-retinoic acid on human SH-SY5Y neuroblastoma as in vitro model in neurotoxicity research. Neurotoxicology 30 (1), 127–135.
- Clark, K.L., George, J.W., Hua, G., Davis, J.S., 2022. Perfluorooctanoic acid promotes proliferation of the human granulosa cell line HGrC1 and alters expression of cell cycle genes and Hippo pathway effector YAP1. Reprod. Toxicol. 110, 49–59.
- Colpan, M.E., Slavin, K.V., 2010. Subthalamic and red nucleus volumes in patients with Parkinson's disease: do they change with disease progression? Park. Relat. Disord. 16 (6), 398–403.
- Constantinescu, R., Constantinescu, A.T., Reichmann, H., Janetzky, B., 2007. In: Gerlach, M., Deckert, J., Double, K., Koutsilieri, E. (Eds.), Neuronal Differentiation and Long-Term Culture of the Human Neuroblastoma Line SH-Sy5y, Neuropsychiatric Disorders an Integrative Approach. Springer Vienna, Vienna, pp. 17–28. Vienna, 2007//.
- Deng, S.-Z., Xu, C.-L., Xu, Z.-F., Zhou, L.-Y., Xie, S.-J., Wei, K.-N., Jin, Y.-C., Zeng, Z.-C., Yang, X.-J., Tan, S.-H., Wang, H.-L., 2021. Perfluorodecanoic acid induces meiotic defects and deterioration of mice oocytes in vitro. Toxicology 460, 152884.
- Di Nisio, A., Pannella, M., Vogiatzis, S., Sut, S., Dall'Acqua, S., Rocca, M.S., Antonini, A., Porzionato, A., De Caro, R., Bortolozzi, M., Toni, L.D., Foresta, C., 2022. Impairment of human dopaminergic neurons at different developmental stages by perfluoro-octanoic acid (PFOA) and differential human brain areas accumulation of perfluoroalkyl chemicals. Environ. Int. 158, 106982.
- Diao, J., Burré, J., Vivona, S., Cipriano, D.J., Sharma, M., Kyoung, M., Südhof, T.C., Brunger, A.T., 2013. Native α-synuclein induces clustering of synaptic-vesicle mimics via binding to phospholipids and synaptobrevin-2/VAMP2. Elife 2, e00592.
- EPA, U., 2016. Drinking Water Health Advisory for Perfluorooctanoic Acid (PFOA). EPA Document 822-R-16-005.
- Fidorra, J., Mielke, T., Booz, J., Feinendegen, L.E., 1981. Cellular and nuclear volume of human cells during the cell cycle. Radiat. Environ. Biophys. 19 (3), 205–214.
- Frost, B., 2016. Alzheimer's disease: an acquired neurodegenerative laminopathy. Nucleus 7 (3), 275–283.
- Gallo, V., Leonardi, G., Genser, B., Lopez-Espinosa, M.-J., Frisbee Stephanie, J., Karlsson, L., Ducatman Alan, M., Fletcher, T., 2012. Serum perfluorooctanoate (PFOA) and perfluorooctane sulfonate (PFOS) concentrations and liver function biomarkers in a population with elevated PFOA exposure. Environ. Health Perspect. 120 (5), 655–660.
- Garnick, L., Massarsky, A., Mushnick, A., Hamaji, C., Scott, P., Monnot, A., 2021. An evaluation of health-based federal and state PFOA drinking water guidelines in the United States. Sci. Total Environ. 761, 144107.

- Ghosh, S., Patel, N., Rahn, D., McAllister, J., Sadeghi, S., Horwitz, G., Berry, D., Wang, K. X., Swerdlow, R.H., 2007. The thiazolidinedione pioglitazone alters mitochondrial function in human neuron-like cells. Mol. Pharmacol. 71 (6), 1695.
- Gillman, M.W., 2005. Developmental origins of health and disease. N. Engl. J. Med. 353 (17), 1848–1850.
- Goyal, D., Limesand, S.W., Goyal, R., 2019. Epigenetic responses and the developmental origins of health and disease. J. Endocrinol. 242 (1), T105–T119.
- H Nataraj, S., T Venkatarangaiah, V., N Subba Rao, A., 2015. Electrochemical surface modification technique to impede mild steel corrosion using perfluorooctanoic acid. J. Electrochem. Sci. Eng. 5 (4), 247–259.
- Haugen, A.C., Schug, T.T., Collman, G., Heindel, J.J., 2014. Evolution of DOHaD: the impact of environmental health sciences. J. Develop. Orig. Health Disease 6 (2), 55-64
- Hu, X.C., Andrews, D.Q., Lindstrom, A.B., Bruton, T.A., Schaider, L.A., Grandjean, P., Lohmann, R., Carignan, C.C., Blum, A., Balan, S.A., Higgins, C.P., Sunderland, E.M., 2016. Detection of poly- and perfluoroalkyl substances (PFASs) in U.S. Drinking water linked to industrial sites, military fire training areas, and wastewater treatment plants. Environ. Sci. Technol. Lett. 3 (10), 344–350.
- Irianto, J., Lee, D.A., Knight, M.M., 2014. Quantification of chromatin condensation level by image processing. Med. Eng. Phys. 36 (3), 412–417.
- Jantzen, C.E., Annunziato, K.M., Cooper, K.R., 2016a. Behavioral, morphometric, and gene expression effects in adult zebrafish (Danio rerio) embryonically exposed to PFOA, PFOS, and PFNA. Aquat. Toxicol. 180, 123–130.
- Jantzen, C.E., Annunziato, K.A., Bugel, S.M., Cooper, K.R., 2016b. PFOS, PFNA, and PFOA sub-lethal exposure to embryonic zebrafish have different toxicity profiles in terms of morphometrics, behavior and gene expression. Aquat. Toxicol. 175, 160–170.
- Javoy-Agid, F., Hirsch, E.C., Dumas, S., Duyckaerts, C., Mallet, J., Agid, Y., 1990.
  Decreased tyrosine hydroxylase messenger RNA in the surviving dopamine neurons of the substantia nigra in Parkinson's disease: an in situ hybridization study.
  Neuroscience 38 (1), 245–253.
- Jin, Z., Liu, Y., 2018. DNA methylation in human diseases. Genes & Diseases 5 (1), 1–8. Kim, H., Hong, M.-W., Bae, Y.-h., Lee, S.-J., 2021. Epigenetic toxicity and cytotoxicity of perfluorooctanoic acid and its effects on gene expression in embryonic mouse hypothalamus cells. Arh. Hig. Rad. Toksikol. 72 (3), 182–189.
- Kingsbury, A.E., Daniel, S.E., Sangha, H., Eisen, S., Lees, A.J., Foster, O.J.F., 2004. Alteration in α-synuclein mRNA expression in Parkinson's disease. Mov. Disord. 19 (2), 162–170.
- Kingsley, S.L., Kelsey, K.T., Butler, R., Chen, A., Eliot, M.N., Romano, M.E., Houseman, A., Koestler, D.C., Lanphear, B.P., Yolton, K., 2017. Maternal serum PFOA concentration and DNA methylation in cord blood: a pilot study. Environ. Res. 158, 174–178.
- Koch, J.C., Bitow, F., Haack, J., d'Hedouville, Z., Zhang, J.N., Tönges, L., Michel, U.,
   Oliveira, L.M.A., Jovin, T.M., Liman, J., Tatenhorst, L., Bähr, M., Lingor, P., 2015.
   Alpha-Synuclein affects neurite morphology, autophagy, vesicle transport and axonal degeneration in CNS neurons. Cell Death Dis. 6 (7) e1811-e1811.
- Korecka, J.A., van Kesteren, R.E., Blaas, E., Spitzer, S.O., Kamstra, J.H., Smit, A.B., Swaab, D.F., Verhaagen, J., Bossers, K., 2013. Phenotypic characterization of retinoic acid differentiated SH-SY5Y cells by transcriptional profiling. PLoS One 8 (5), e63862.
- Kozina, E.A., Khakimova, G.R., Khaindrava, V.G., Kucheryanu, V.G., Vorobyeva, N.E., Krasnov, A.N., Georgieva, S.G., Kerkerian-Le Goff, L., Ugrumov, M.V., 2014. Tyrosine hydroxylase expression and activity in nigrostriatal dopaminergic neurons of MPTP-treated mice at the presymptomatic and symptomatic stages of parkinsonism. J. Neurol. Sci. 340 (1), 198–207.
- Lee, J., Escher, B.I., Scholz, S., Schlichting, R., 2022. Inhibition of neurite outgrowth and enhanced effects compared to baseline toxicity in SH-SY5Y cells. Arch. Toxicol. 96 (4) 1039–1053
- Li, P., Marshall, L., Oh, G., Jakubowski, J.L., Groot, D., He, Y., Wang, T., Petronis, A., Labrie, V., 2019. Epigenetic dysregulation of enhancers in neurons is associated with Alzheimer's disease pathology and cognitive symptoms. Nat. Commun. 10 (1), 2246.
- Lin, L.F., Xie, J., Sánchez, O.F., Bryan, C., Freeman, J.L., Yuan, C., 2021. Low dose lead exposure induces alterations on heterochromatin hallmarks persisting through SH-SY5Y cell differentiation. Chemosphere 264, 128486.
- Liu, W., Irudayaraj, J., 2020. Perfluorooctanoic acid (PFOA) exposure inhibits DNA methyltransferase activities and alters constitutive heterochromatin organization. Food Chem. Toxicol. 141, 111358.
- Liu, Y., Eliot Melissa, N., Papandonatos George, D., Kelsey Karl, T., Fore, R., Langevin, S.,
   Buckley, J., Chen, A., Lanphear Bruce, P., Cecil Kim, M., Yolton, K., Hivert, M.-F.,
   Sagiv Sharon, K., Baccarelli Andrea, A., Oken, E., Braun Joseph, M., 2022.
   Gestational perfluoroalkyl substance exposure and DNA methylation at birth and 12
   Years of age: a longitudinal epigenome-wide association study. Environ. Health
   Perspect. 130 (3), 037005.
- Lopes, F.M., Londero, G.F., de Medeiros, L.M., da Motta, L.L., Behr, G.A., de Oliveira, V. A., Ibrahim, M., Moreira, J.C.F., de Oliveira Porciúncula, L., da Rocha, J.B.T., Klamt, F., 2012. Evaluation of the neurotoxic/neuroprotective role of organoselenides using differentiated human neuroblastoma SH-SY5Y cell line challenged with 6-hydroxydopamine. Neurotox. Res. 22 (2), 138–149.
- Ma, Y., Yang, J., Wan, Y., Peng, Y., Ding, S., Li, Y., Xu, B., Chen, X., Xia, W., Ke, Y., Xu, S., 2018. Low-level perfluorooctanoic acid enhances 3 T3-L1 preadipocyte differentiation via altering peroxisome proliferator activated receptor gamma expression and its promoter DNA methylation. J. Appl. Toxicol. 38 (3), 398–407.
- Mastroeni, D., Grover, A., Leonard, B., Joyce, J.N., Coleman, P.D., Kozik, B., Bellinger, D. L., Rogers, J., 2009. Microglial responses to dopamine in a cell culture model of Parkinson's disease. Neurobiol. Aging 30 (11), 1805–1817.

- Miglio, G., Rosa, A.C., Rattazzi, L., Collino, M., Lombardi, G., Fantozzi, R., 2009. PPARγ stimulation promotes mitochondrial biogenesis and prevents glucose deprivationinduced neuronal cell loss. Neurochem. Int. 55 (7), 496–504.
- Miura, R., Araki, A., Miyashita, C., Kobayashi, S., Kobayashi, S., Wang, S.-L., Chen, C.-H., Miyake, K., Ishizuka, M., Iwasaki, Y., 2018. An epigenome-wide study of cord blood DNA methylations in relation to prenatal perfluoroalkyl substance exposure: the Hokkaido study. Environ. Int. 115, 21–28.
- Mogensen, U.B., Grandjean, P., Nielsen, F., Weihe, P., Budtz-Jørgensen, E., 2015. Breastfeeding as an exposure pathway for perfluorinated alkylates. Environ. Sci. Technol. 49 (17), 10466–10473.
- Mu, M.-D., Qian, Z.-M., Yang, S.-X., Rong, K.-L., Yung, W.-H., Ke, Y., 2020. Therapeutic effect of a histone demethylase inhibitor in Parkinson's disease. Cell Death Dis. 11 (10) 927
- Narendra, D.P., Jin, S.M., Tanaka, A., Suen, D.-F., Gautier, C.A., Shen, J., Cookson, M.R., Youle, R.J., 2010. PINK1 is selectively stabilized on impaired mitochondria to activate Parkin. PLoS Biol. 8 (1), e1000298.
- Neystat, M., Lynch, T., Przedborski, S., Kholodilov, N., Rzhetskaya, M., Burke, R.E., 1999. α-Synuclein expression in substantia nigra and cortex in Parkinson's disease. Mov. Disord. 14 (3), 417–422.
- OECD, 2018. Toward a New Comprehensive Global Database of Per-And Polyfluoroalkyl Substances (PFASs): Summary Report on Updating the OECD 2007 List of Per and Polyfluoroalkyl Substances (PFASs).
- Oka, S., Alcendor, R., Zhai, P., Park, Ji Y., Shao, D., Cho, J., Yamamoto, T., Tian, B., Sadoshima, J., 2011. PPARα-Sirt1 complex mediates cardiac hypertrophy and failure through suppression of the ERR transcriptional pathway. Cell Metabol. 14 (5), 508-611
- Panagaki, D., Croft Jacob, T., Keuenhof, K., Larsson Berglund, L., Andersson, S., Kohler, V., Büttner, S., Tamás Markus, J., Nyström, T., Neutze, R., Höög Johanna, L., 2021. Nuclear envelope budding is a response to cellular stress. Proc. Natl. Acad. Sci. USA 118 (30), e2020997118.
- Paustenbach, D.J., Panko, J.M., Scott, P.K., Unice, K.M., 2006. A methodology for estimating human exposure to perfluorooctanoic acid (PFOA): a retrospective exposure assessment of a community (1951–2003). J. Toxicol. Environ. Health, Part A 70 (1), 28–57.
- Pezzini, F., Bettinetti, L., Di Leva, F., Bianchi, M., Zoratti, E., Carrozzo, R., Santorelli, F. M., Delledonne, M., Lalowski, M., Simonati, A., 2017. Transcriptomic profiling discloses molecular and cellular events related to neuronal differentiation in SH-SY5Y neuroblastoma cells. Cell. Mol. Neurobiol. 37 (4), 665–682.
- Pieper, H.C., Evert, B.O., Kaut, O., Riederer, P.F., Waha, A., Wüllner, U., 2008. Different methylation of the TNF-alpha promoter in cortex and substantia nigra: implications for selective neuronal vulnerability. Neurobiol. Dis. 32 (3), 521–527.
- Pierozan, P., Jerneren, F., Karlsson, O., 2018. Perfluorooctanoic acid (PFOA) exposure promotes proliferation, migration and invasion potential in human breast epithelial cells. Arch. Toxicol. 92 (5), 1729–1739.
- Pierozan, P., Cattani, D., Karlsson, O., 2020. Perfluorooctane sulfonate (PFOS) and perfluorooctanoic acid (PFOA) induce epigenetic alterations and promote human breast cell carcinogenesis in vitro. Arch. Toxicol. 94 (11), 3893–3906.
- Rashid, F., Ramakrishnan, A., Fields, C., Irudayaraj, J., 2020. Acute PFOA exposure promotes epigenomic alterations in mouse kidney tissues. Toxicol Rep 7, 125–132.
- Roca-Cusachs, P., Alcaraz, J., Sunyer, R., Samitier, J., Farré, R., Navajas, D., 2008. Micropatterning of single endothelial cell shape reveals a tight coupling between nuclear volume in G1 and proliferation. Biophys. J. 94 (12), 4984–4995.
- Sachs, M., Onodera, C., Blaschke, K., Ebata, Kevin T., Song, Jun S., Ramalho-Santos, M., 2013. Bivalent chromatin marks developmental regulatory genes in the mouse embryonic germline in vivo. Cell Rep. 3 (6), 1777–1784.
- Salimi, A., Nikoosiar Jahromi, M., Pourahmad, J., 2019. Maternal exposure causes mitochondrial dysfunction in brain, liver, and heart of mouse fetus: an explanation for perfluorooctanoic acid induced abortion and developmental toxicity. Environ. Toxicol. 34 (7), 878–885.
- Schapira, A.H.V., Cooper, J.M., Dexter, D., Clark, J.B., Jenner, P., Marsden, C.D., 1990. Mitochondrial complex I deficiency in Parkinson's disease. J. Neurochem. 54 (3), 823–827.
- Schooley, A., Vollmer, B., Antonin, W., 2012. Building a nuclear envelope at the end of mitosis: coordinating membrane reorganization, nuclear pore complex assembly, and chromatin de-condensation. Chromosoma 121 (6), 539–554.
- Shah, P., Hobson, C.M., Cheng, S., Colville, M.J., Paszek, M.J., Superfine, R., Lammerding, J., 2021. Nuclear deformation causes DNA damage by increasing replication stress. Curr. Biol. 31 (4), 753–765 e6.
- Shipley, M.M., Mangold, C.A., Szpara, M.L., 2016. Differentiation of the SH-SY5Y human neuroblastoma cell line. JoVE: JoVE 108.
- Souders, C.L., Sanchez, C.L., Malphurs, W., Aristizabal-Henao, J.J., Bowden, J.A., Martyniuk, C.J., 2021. Metabolic profiling in human SH-SY5Y neuronal cells exposed to perfluorooctanoic acid (PFOA). Neurotoxicology 85, 160–172.

- Stephens, A.D., Liu, P.Z., Banigan, E.J., Almassalha, L.M., Backman, V., Adam, S.A., Goldman, R.D., Marko, J.F., 2018. Chromatin histone modifications and rigidity affect nuclear morphology independent of lamins. Mol. Biol. Cell 29 (2), 220–233.
- Su, X., Fischer, D.L., Li, X., Bankiewicz, K., Sortwell, C.E., Federoff, H.J., 2017. Alphasynuclein mRNA is not increased in sporadic PD and alpha-synuclein accumulation does not block GDNF signaling in Parkinson's disease and disease models. Mol. Ther. 25 (10), 2231–2235.
- Sunderland, E.M., Hu, X.C., Dassuncao, C., Tokranov, A.K., Wagner, C.C., Allen, J.G., 2019. A review of the pathways of human exposure to poly-and perfluoroalkyl substances (PFASs) and present understanding of health effects. J. Expo. Sci. Environ. Epidemiol. 29 (2), 131–147.
- Tsika, E., Kannan, M., Foo, C.S.-Y., Dikeman, D., Glauser, L., Gellhaar, S., Galter, D., Knott, G.W., Dawson, T.M., Dawson, V.L., Moore, D.J., 2014. Conditional expression of Parkinson's disease-related R1441C LRRK2 in midbrain dopaminergic neurons of mice causes nuclear abnormalities without neurodegeneration. Neurobiol. Dis. 71, 345–358.
- Tukker, A.M., Bouwman, L.M.S., van Kleef, R.G.D.M., Hendriks, H.S., Legler, J., Westerink, R.H.S., 2020. Perfluorooctane sulfonate (PFOS) and perfluorooctanoate (PFOA) acutely affect human  $\alpha1\beta2\gamma2L$  GABAA receptor and spontaneous neuronal network function in vitro. Sci. Rep. 10 (1), 5311.
- Valente, A.J., Maddalena, L.A., Robb, E.L., Moradi, F., Stuart, J.A., 2017. A simple ImageJ macro tool for analyzing mitochondrial network morphology in mammalian cell culture. Acta Histochem. 119 (3), 315–326.
- Vashishtha, M., Ng Christopher, W., Yildirim, F., Gipson Theresa, A., Kratter Ian, H., Bodai, L., Song, W., Lau, A., Labadorf, A., Vogel-Ciernia, A., Troncosco, J., Ross Christopher, A., Bates Gillian, P., Krainc, D., Sadri-Vakili, G., Finkbeiner, S., Marsh, J.L., Housman David, E., Fraenkel, E., Thompson Leslie, M., 2013. Targeting H3K4 trimethylation in Huntington disease. Proc. Natl. Acad. Sci. USA 110 (32), E3027—E3036.
- Voelker, D.R., 2004. Lipid synthesis and transport in mitochondrial biogenesis. In: Mitochondrial Function and Biogenesis. Springer Berlin Heidelberg, Berlin, Heidelberg, pp. 267–291.
- von Schimmelmann, M., Feinberg, P.A., Sullivan, J.M., Ku, S.M., Badimon, A., Duff, M.K., Wang, Z., Lachmann, A., Dewell, S., Ma'ayan, A., Han, M.-H., Tarakhovsky, A., Schaefer, A., 2016. Polycomb repressive complex 2 (PRC2) silences genes responsible for neurodegeneration. Nat. Neurosci. 19 (10), 1321–1330.
- Wang, Z., DeWitt, J.C., Higgins, C.P., Cousins, I.T., 2017. A Never-Ending Story of Per-And Polyfluoroalkyl Substances (PFASs)? ACS Publications.
- Wang, P., Dreger, M., Madrazo, E., Williams Craig, J., Samaniego, R., Hodson Nigel, W.,
   Monroy, F., Baena, E., Sánchez-Mateos, P., Hurlstone, A., Redondo-Muñoz, J., 2018.
   WDR5 modulates cell motility and morphology and controls nuclear changes induced by a 3D environment. Proc. Natl. Acad. Sci. USA 115 (34), 8581–8586.
- Wen, Y., Mirji, N., Irudayaraj, J., 2020a. Epigenetic toxicity of PFOA and GenX in HepG2 cells and their role in lipid metabolism. Toxicol. Vitro 65, 104797.
- Wen, Y., Chen, J., Li, J., Arif, W., Kalsotra, A., Irudayaraj, J., 2020b. Effect of PFOA on DNA methylation and alternative splicing in mouse liver. Toxicol. Lett. 329, 38–46.
- Weng, Z., Xu, C., Zhang, X., Pang, L., Xu, J., Liu, Q., Zhang, L., Xu, S., Gu, A., 2020. Autophagy mediates perfluorooctanoic acid-induced lipid metabolism disorder and NLRP3 inflammasome activation in hepatocytes. Environ. Pollut. 267, 115655.
- Wolf, C.J., Takacs, M.L., Schmid, J.E., Lau, C., Abbott, B.D., 2008. Activation of mouse and human peroxisome Proliferator—Activated receptor alpha by perfluoroalkyl acids of different functional groups and chain lengths. Toxicol. Sci. 106 (1), 162-171
- Xie, J., Lin, L., Sánchez, O.F., Bryan, C., Freeman, J.L., Yuan, C., 2021. Pre-differentiation exposure to low-dose of atrazine results in persistent phenotypic changes in human neuronal cell lines. Environ. Pollut. 271, 116379.
- Xu, B., Ji, X., Chen, X., Yao, M., Han, X., Chen, M., Tang, W., Xia, Y., 2015. Effect of perfluorooctane sulfonate on pluripotency and differentiation factors in mouse embryoid bodies. Toxicology 328, 160–167.
- Yin, X., Li, L., Zhang, X., Yang, Y., Chai, Y., Han, X., Feng, Z., 2013. Development of neural stem cells at different sites of fetus brain of different gestational age. Int. J. Clin. Exp. Pathol. 6 (12), 2757–2764.
- Yu, N., Wei, S., Li, M., Yang, J., Li, K., Jin, L., Xie, Y., Giesy, J.P., Zhang, X., Yu, H., 2016. Effects of perfluoroctanoic acid on metabolic profiles in brain and liver of mouse revealed by a high-throughput targeted metabolomics approach. Sci. Rep. 6 (1), 23963.
- Yu, T., Zhou, G., Cai, Z., Liang, W., Du, Y., Wang, W., 2021. Behavioral effects of early-life exposure to perfluorooctanoic acid might synthetically link to multiple aspects of dopaminergic neuron development and dopamine functions in zebrafish larvae. Aquat. Toxicol. 238, 105926.
- Zheng, G., Schreder, E., Dempsey, J.C., Uding, N., Chu, V., Andres, G., Sathyanarayana, S., Salamova, A., 2021. Per- and polyfluoroalkyl substances (PFAS) in breast milk: concerning trends for current-use PFAS. Environ. Sci. Technol. 55 (11), 7510–7520.